JOURNAL OF PROPULSION AND POWER
Vol. 18, No. 2, March–April 2002

Technical Notes

TECHNICAL NOTES are short manuscripts describing new developments or important results of a preliminary nature. These Notes cannot exceed 6 manuscript pages and 3 figures; a page of text may be substituted for a figure and vice versa. After informal review by the editors, they may be published within a few months of the date of receipt. Style requirements are the same as for regular contributions (see inside back cover).

Correlating Laser Induced Fluorescence and Molecular Beam Mass Spectrometry Ion Energy Distributions

George J. Williams,* Timothy B. Smith,*
Frank S. Gulczinski,* and Alec D. Gallimore†
University of Michigan, Ann Arbor, Michigan 48109

Introduction

SEVERAL recent investigations have measured the ion temperature and the full width at half maximum (FWHM) of the ion energy distribution in a variety of electric propulsion systems.[1–8] Significant attention has been paid to the apparent discrepancy between the spread in ion energy distributions measured using laser-induced fluorescence (LIF) and those obtained using other diagnostic techniques. Though the energy and velocity distributions are widely acknowledged to be non-Maxwellian, temperatures calculated from Maxwellian fits to the distributions are commonly used as a figure of merit in the comparisons of distributions.[1–3,5,8] Several explanations have been suggested to resolve the order of magnitude difference between the temperature indicated by LIF measurements (a few electron volts) and the FWHM of ion energy distributions measured by energy analyzers (tens of electron volts). These include the collecting of crossflowing ions in probes, nonrepresentative sampling of the velocity distribution by LIF, broadening by multiply charged ions that are absent from LIF measurements, and collisional broadening by the intrusive nature of probe measurements.

LIF and energy analyzer data were taken at the same location in the plume of the 5-kW P5 Hall thruster to provide a concrete comparison of ion energy and velocity distributions, as well as temperatures from the two techniques. All testing was conducted in the large vacuum test facility at the Plasmadynamics and Electric Propulsion Laboratory.[5]

Theory

LIF

Dual-beam interrogation of the plasma enabled simultaneous measurement of azimuthal and axial velocity distributions.[5,9] The laser beams are split just downstream of the dye laser, propagate downstream parallel, enter the vacuum chamber, and pass through a 10-cm-diam lens.[6] The azimuthal beam passes through the center of the lens and is focused at the interrogation point. The axial beam passes near the edge of the lens, is refracted at an angle α, and crosses the azimuthal beam, focused, at the same interrogation point. The volume of interrogation, which is defined by the crossing of the laser beams, is roughly 1 mm^3.

A first-order fit to the fluorescence spectrum provides the mean velocity and temperature in the azimuthal and off-axis directions. The line-fitting model considers only Doppler broadening of a nonstationary Maxwellian distribution, which yields a Gaussian line shape,[10] where ν_0 is the line center, M the mass of the ion, and $\Delta\nu_D$ the FWHM:

$$\Delta\nu_D = (2\nu_0/c)[2\ln(2)kT/M]^{\frac{1}{2}} \tag{1}$$

The Xe II LIF spectrum of a low-temperature reference cell is curve fitted with six Gaussians with identical widths, whose line centers and relative line strengths are chosen to provide the best fit to the data.[6] The fits to determine temperatures have an uncertainty of roughly ± 0.1 eV. The mean axial velocity is given by

$$v_A = \frac{v_0 - v_R\cos(\alpha)}{\sin(\alpha)} \tag{2}$$

where $\alpha = 9.72 \pm 0.04$ deg. Because the azimuthal and axial velocity distributions are statistically independent, the axial temperature T_A is given by the elliptical relationship[11]

$$\left(\frac{T_R}{T_0}\right)^2 = \cos^2\left(\frac{\pi}{2} - \alpha\right) + \left(\frac{T_R}{T_A}\right)^2 \sin^2\left(\frac{\pi}{2} - \alpha\right) \tag{3}$$

or, solving for T_A

$$T_A = T_R\left[\frac{(T_R/T_0)^2 - 1}{\cos^2(\alpha)} + 1\right]^{-\frac{1}{2}} \tag{4}$$

where T_R is the temperature of the azimuthal distribution and T_0 is the temperature of the off-axis distribution. The equivalent energy distribution $f(E)$ for a given component can then be calculated directly from the velocity distribution $f(v)$, where $E = Mv^2/2e$.

MBMS

The molecular beam mass spectrometer (MBMS) is a time-of-flight mass spectrometer with a 45-deg parallel plate energy analyzer. Ions pass into the MBMS through a sampling orifice and enter the 45-deg energy analyzer, which allows only ions of a specific energy-to-chargeratio to pass through and reach the detector.[1,3] This ratio is selected by setting the electric field between the plates of the analyzer. Sweeping the value of this field yields an entire ion energy distribution.

The MBMS, unlike LIF, directly records the axial ion energy distribution function. A drifting Maxwellian energy distribution has the form[10]

$$f(E) = \left(\frac{1}{4\pi kTE}\right)^{\frac{1}{2}} \exp\left\{-\frac{M}{2kT}\left(\sqrt{\frac{2E}{M}} - \sqrt{\frac{2E_m}{M}} - \frac{kT}{M}\sqrt{\frac{M}{2E_m}}\right)^2\right\} \tag{5}$$

The temperature of the distribution can be calculated in terms of the ratio $r = \sqrt{(E_{1/e}E_m)}$:

Received 27 September 1999; revision received 1 September 2001; accepted for publication 19 September 2001.

*Graduate Student, Plasmadynamics and Electric Propulsion Laboratory.
†Associate Professor and Director, Department of Aerospace Engineering. Associate Fellow AIAA.

$$T[\mathrm{eV}] = \frac{(r-1)^2}{r - \ell n(r)} E_m[\mathrm{V}] \tag{6}$$

where $E_{1/e}$ is the energy at the $1/e$ point of the energy distribution. The velocity distribution is then directly calculated for each energy in the distribution.

Velocity and Energy Distributions

Collisionless acceleration of an ion beam tends to cool the velocity distribution along the acceleration axis.[12,13] Consider an ion population with initial bulk velocity u_0 and velocity FWHM, Δu_0. A potential drop U will accelerate a stationary ion mass M to $u_e = \sqrt{(2eU/M)}$, while ions at the FWHM points of the initial distribution will be accelerated to

$$u_\pm = \sqrt{(u_0 \pm \Delta u_0/2)^2 + u_0^2}$$

For $u_e \gg u_0$, the FWHM of the accelerated beam is $\Delta u_f = u_+ - u_- \equiv \Delta u_0 u_0/u_e$. Because $\Delta u_0 = 2\sqrt{[2\,\ell n(2) kT_0/M]}$, the ratio of the final to initial axial temperatures becomes

$$T_f/T_0 = (\Delta u_f/\Delta u_0)^2 = (u_0/u_e)^2 \tag{7}$$

and the Doppler-broadened axial linewidth becomes

$$\Delta\nu_D = (2\nu_0/c)(u_0/u_e)[2\,\ell n(2)(kT_0/M)]^{\frac{1}{2}} \tag{8}$$

Thus [by use of Eq. (8)], accelerating a population initially at 300 m/s and 5800 K through 250 V would result in an axial velocity of 19.2 km/s and an axial temperature of 1.36 K. The azimuthal temperature and linewidth remain unaffected by this process.

Values of the ratio of electric field strength (volts per centimeter) to total number density (per cubic centimeter), ε/N, less than 5×10^{-16} (Vcm^2) indicate a collisionally dominated flow.[11] For an Xe flow rate of 60 cm^3/s and, from LIF, a temperature of 4300 K, ε/N is roughly 8×10^{-15} (Vcm^2). Thus, the assumption of a purely displaced Maxwellian distribution is not strictly appropriate.

Electron–ion collisions could occur to restore temperature isotropy. Given an ion density n_0, upstream of the acceleration zone, an electron temperature T_e, and assuming $U \gg T_e$, the mean free path for electron–ion momentum transfer collisions λ is

$$\lambda = \frac{1}{n_0\sigma_m}\left(\frac{3\pi}{8}\frac{M_e}{M}\frac{U}{T_e}\frac{2eU}{Mu_0^2}\right)^{\frac{1}{2}} \tag{9}$$

where M_e is the electron mass, σ_m is the momentum transfer cross section, and u_0 is the initial ion bulk velocity before electrostatic acceleration.[10] For $n_0 = 1 \times 10^{13}$ cm^{-3} and $\sigma_m = 2 \times 10^{-14}$ cm^2, $\lambda \approx 0.5$ cm, which is of the same order of magnitude as the acceleration length.[5,14] Thus, some restoration to equilibrium should be expected.

Divergence of the beam within the interrogation spot would also tend to counteract this cooling effect. Given a divergence angle θ within the spot and a sufficiently cooled beam so that $f(v) = \delta(v-u)$, the divergence linewidth is[11]

$$\Delta\nu_{\mathrm{div}} = (u_e/c)[1 - \cos(\theta/2)]\nu_0 \tag{10}$$

which translates to an equivalent temperature increase, ΔT_{div},

$$\Delta T_{\mathrm{div}} = \frac{1}{2\,\ell n(2)}\frac{M}{k}\left\{\frac{u_e}{2}\left[1 - \cos\left(\frac{\theta}{2}\right)\right]\right\}^2 \tag{11}$$

For example, given the same initial temperature of 5800 K, a potential drop of 250 V, and a beam divergence of 40 deg across the interrogation spot results in an apparent temperature increase of 3800–9600 K. A 4-deg beam divergence gives an apparent temperature increase of only 0.0038 K or, roughly, the same 5800 K.

Results and Discussion

Figure 1 shows LIF and MBMS data taken 0.1 m downstream of the center of the P5 discharge annulus with the P5 operating at 300 V, 5.3 A, and a 6 mg/s Xe flow rate. The three LIF spectra (axial, azimuthal, and reference cell) in Fig. 1a were taken simultaneously. Shifts away from the reference cell peak indicate increasing speed. From curve fits and using Eq. (4), ion temperatures of these data were 6500, 4300, and 750 K for the axial, azimuthal, and reference cell distributions, respectively. The difference in axial and azimuthal temperatures may indicate beam divergence. The LIF axial velocity distribution peaked at 17.6 ± 1.5 km/s [from Eq. (2)]; the corresponding energy distribution peak is at 210 ± 20 eV with a FWHM of 25 eV.

Though the azimuthal and axial velocity distributions (Fig. 1b) have roughly the same breadth, the axial and azimuthal energy distributions (Fig. 1c) are radically different. The peak of the azimuthal velocity profile is at -750 m/s, which corresponds to an energy of 0.4 eV. This illustrates that, for roughly the same temperature, the FWHM of the energy distribution is a function of the energy of the peak in that distribution. As the bulk ion energy increases, so will the breadth of the distribution.

Figures 1b and 1c present MBMS data in addition to distributions calculated from LIF data. Note that there is a second peak in the MBMS distributions that is not captured in the LIF traces. This

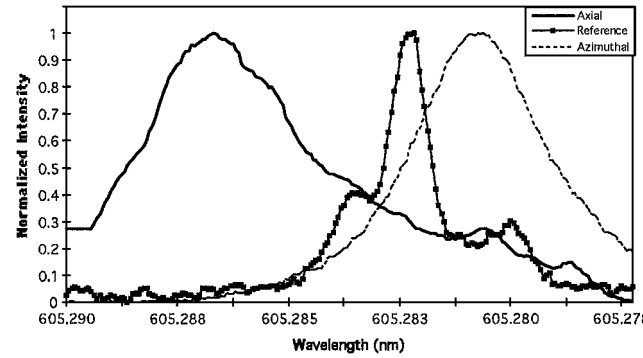

a) LIF spectra

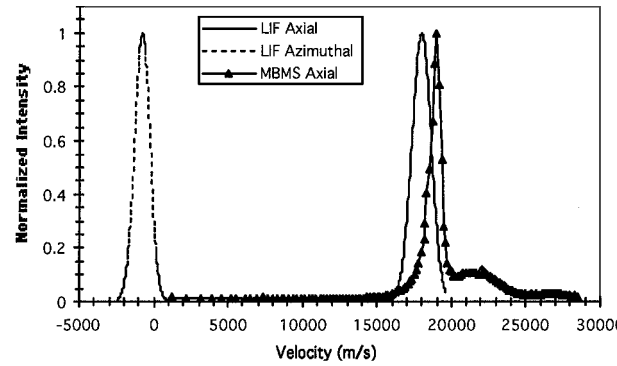

b) Velocity distributions

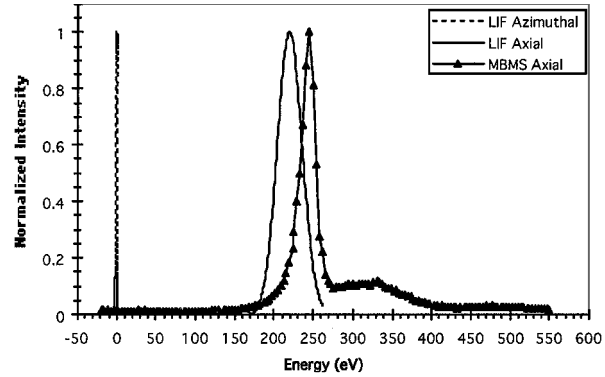

c) Energy distributions

Fig. 1 Wavelength, velocity, and energy distributions for 1.5-kW P5 operation; data taken 0.1 m downstream in center of discharge annulus.

may result from elastic momentum transfer or charge exchange collisions. This second distribution is obscured in the LIF spectra by broadening and hyperfine structure. For this analysis, only the characteristics of the larger peak in the MBMS energy distribution were considered.

The MBMS velocity distribution peaked at 18.9 ± 0.4 km/s, and the energy distribution peaked at 230 ± 10 eV corrected for plasma potential with a FWHM of 20 eV. The bulk axial velocity given by LIF is 7.4% less than the MBMS peak velocity. This difference is too great for the uncertainty in angle α. The difference may result from noise-related fitting errors of the LIF data (potentially as large as 10% uncertainty, or 1500 m/s), incorrect estimation of the plasma potential in the MBMS data reduction, chamber effects in the MBMS data, or a combination of these. Applying Eq. (6) to the MBMS energy distribution yields a temperature of 2500 K.

Neither axial temperature measurement shows the drastic cooling predicted by collisionless acceleration theory. From Eq. (11), a divergence of 35 ± 6 deg, which is consistent with LIF velocity mapping off the centerline of the discharge annulus,[5] yields the temperature measured by LIF. Beam divergence, plasma oscillations, and electron-neutral collisions may also offset any acceleration cooling, and the measured temperature probably results from a complex combination of effects.

The MBMS temperature is roughly 41% of the LIF axial temperature. This difference may result from the non-Maxwellian nature of the data and/or saturation broadening of the LIF data. Whereas the scarcity of data in the MBMS peak introduces uncertainty in the evaluation of Eq. (5), a distribution with a temperature of 6500 K is a poor fit of the data. An improved deconvolution model is needed to increase the accuracy of velocity and energy distributions measured with LIF.

Conclusions

The spread in the ion energy distribution obtained from LIF data is comparable to that obtained from MBMS data given the uncertainties in both techniques involved. The ion temperatures calculated from the two techniques were of the same order of magnitude and indicate significant beam divergence. The primary differences associated with these techniques that are stated in the literature are not actually present. The MBMS is not artificially broadening the signal due to the collection of crossflowing ions, and the LIF signal is neither from a sparsely populated electronic state nor from an interrogation spot too small to capture the velocity profile.

References

[1]King, L. B., and Gallimore, A. D., "Transport-Property Measurements in the Plume of an SPT-100 Hall Thruster," *Journal of Propulsion and Power*, Vol. 14, No. 3, 1998, pp. 327–335.

[2]Manzella, D. H., "Stationary Plasma Thruster Ion Velocity Distribution," AIAA Paper 94-3141, June 1994.

[3]Gulczinski, F. S., and Gallimore, A. D., "Near-Field Ion Energy and Species Measurements of a 5-kW Laboratory Hall Thruster," AIAA Paper 99-2430, June 1999.

[4]Domonkos, M. T., Marrese, C. M., Haas, J. M., and Gallimore, A. D., "Very Near-Field Plume Investigation of the D-55," AIAA Paper 97-3062, July 1997.

[5]Williams, G. J., Smith, T. B., Gulczinski, F. S., Beal, B. E., Gallimore, A. D., and Drake, R. P., "Laser-Induced Fluorescence Measurement of Ion Velocities in the Plume of a Hall Effect Thruster," AIAA Paper 99-2424, June 1999.

[6]Williams, G. J., Smith, T. B., Gulczinski, F. S., Beal, B. E., Gallimore, A. D., and Drake, R. P., "Laser-Induced Fluorescence Characterization of Ions Emitted from Hollow Cathodes," AIAA Paper 99-2862, June 1999.

[7]Kameyama, I., and Wilbur, J. P., "Characteristics of Ions Emitted from High-Current Hollow Cathodes," *Proceedings of the International Electric Propulsion Conference*, IEPC Paper 93-023, Aug. 1993.

[8]Hargus, W. A., and Cappelli, M. A., "Interior and Exterior Laser-Induced Fluorescence and Plasma Potential Measurements on a Laboratory Hall Thruster," AIAA Paper 99-2721, June 1999.

[9]Keefer, D., Wright, N., Hornkohl, J., and Bangasser, J., "Multiplexed LIF and Langmuir Probe Diagnostic Measurements in the TAL D-55 Thruster," AIAA Paper 99-2425, June 1999.

[10]Gombosi, T. I., *Gaskinetic Theory*, Cambridge Univ. Press, New York, 1994, pp. 39, 40.

[11]Dressler, R. A., Beijers, J. P. M., Meyer, H., Penn, S. M., Bierbaum, V. M., and Leone, S. R., "Laser Probing of Ion Velocity Distributions in Drift Fields: Parallel and Perpendicular Temperatures and Mobility for Ba^+ in He," *Journal of Chemical Physics*, Vol. 89, No. 8, 1988, p. 4707.

[12]Kaufman, S. L., "High-Resolution Laser Spectroscopy in Fast Beams," *Optics Communications*, Vol. 17, No. 3, 1976, pp. 309–312.

[13]Meehan, N. B., Schmidt, D. P., Hargus, W. A., and Cappelli, M. A., "Optical Study of Anomalous Electron Transport in a Laboratory Hall Thruster," AIAA Paper 99-2284, June 1999.

[14]Haas, J. M., and Gallimore, A. D., "An Investigation of Internal Ion Number Density and Electron Temperature Profiles in a Laboratory-Model Hall Thruster," AIAA Paper 2000-3422, July 2000.

Transonic Rotor Blade Pressure Measurement Using Fluorescent Paints

T. Liu*
NASA Langley Research Center, Hampton, Virginia 23681
S. Torgerson†
LM Aero, Palmdale, California 93550
J. Sullivan‡
Purdue University, West Lafayette, Indiana 47907
R. Johnston§
Pratt & Whitney, Middletown, Connecticut 06457
and
S. Fleeter¶
Purdue University, West Lafayette, Indiana 47907

Nomenclature

A	=	constant in Stern–Volmer relation
B	=	constant in Stern–Volmer relation
C	=	rotor chord
E	=	Arrhenius activation energy
I	=	measured luminescent intensity
p	=	pressure
R	=	radial location
Rg	=	universal gas constant
T	=	temperature, K
X	=	chordwise distance

Subscripts

hub	=	value at hub location
ref	=	reference value
0	=	stagnation value

Introduction

PRESSURE and temperature-sensitive paints have been utilized for the measurement of blade surface pressure and temperature in a high-speed axial compressor environment. Four blades were painted: two with temperature sensitive paints and two with pressure sensitive paints allowing pressure distributions to be corrected for paint sensitivity to temperature variations. Pressure maps on the

Received 16 September 2000; revision received 5 July 2001; accepted for publication 20 October 2001.

*Research Scientist, Model Systems. Member AIAA.
†Engineer, Test. Member AIAA.
‡Professor, School of Aeronautics and Astronautics. Senior Member AIAA.
§Instrumentation Technology Manager. Senior Member AIAA.
¶McAllister Distinguished Professor, School of Mechanical Engineering. Fellow AIAA.